

Effect of the vacancy interaction on the antiphase domain growth process in a two dimensional binary alloy

Marcel Porta, Carlos Frontera, Eduard Vives and Teresa Castán

*Departament d'Estructura i Constituents de la Matèria, Facultat de Física,
Universitat de Barcelona, Diagonal 647, E-08028 Barcelona, Catalonia, Spain.*

(October 6, 2018)

Abstract

We have performed a Monte Carlo simulation study of the influence of diffusing vacancies on the antiphase domain growth process in a binary alloy after a quench through an order-disorder transition. The problem has been modeled by means of a Blume-Emery-Griffiths hamiltonian which biquadratic coupling parameter K , controls the microscopic interactions between vacancies. The asymmetric term L has been taken $L = 0$ and the ordering dynamics has been studied at very low temperature as function of K inside the range $-0.5 \leq K/J \leq 1.40$ (with $J > 0$ being the ordering energy). The system evolves according to the Kawasaki dynamics which conserves the alloy concentration while the order parameter does not. The simulations have been performed on a two-dimensional square lattice and the concentration has been taken so that the system corresponds to an stoichiometric alloy with small concentration of vacancies. We obtain that, independently of K , the vacancies exhibit a tendency to concentrate at the antiphase boundaries. This effect gives rise, via the vacancy-vacancy interaction (described by K), to an effective interaction between bulk diffusing vacancies and moving interfaces which turns out to strongly influence the domain growth process. One dis-

tinguishes three different behaviors: *i*) For $K/J < 1$ the growing process of ordered domains is anisotropic and can be described by algebraic laws with effective exponents lower than $1/2$; *ii*) $K/J \simeq 1$ corresponds to the standard Allen-Cahn growth; *iii*) for $K/J > 1$ we found that, although the motion of the interface is curvature-driven, the repulsive effective interaction between both the vacancies in the bulk and those at the interfaces provokes a slow down of the growth.

PACS numbers: 05.70.Ln, 64.60.Cn, 61.50.Ks, 61.70.Yq

I. INTRODUCTION

The dynamical evolution of a binary alloy after a quench from a high temperature disordered phase has been one of the prototypes in the study of relaxational processes towards equilibrium. It has been found that the late stages of this process obey dynamical scaling and the typical domain size $R(t)$ dominates all other lengths [1,2]. In this regime, the domains grow in time according to a power-law $R(t) \sim t^x$ with the growth exponent x satisfying a remarkable universality. For the case of a pure, ideal system, the exponent $x = 1/2$ [3] is associated with cases where the order parameter is not conserved, whereas $x = 1/3$ [4] describes systems with conserved order parameter. For the non-conserved case a typical example is a binary alloy undergoing an order-disorder phase transition. Most theoretical studies are limited to ideal conditions, that is to a pure, stoichiometric binary alloy. In such conditions, theory [3] and numerical simulations [5–8] definitively agree about the value of the kinetic exponent $x = 1/2$. Much less unanimity is obtained from the experiments. This is certainly due to the imperfections always present in real materials. Examples are: vacancies, third-component impurities [9], non-stoichiometry [10], dislocations, etc... It is of great interest to elucidate in which manner and to what extent the presence of these imperfections modifies the ideal asymptotic growth-law.

We shall not consider here the problem of quenched disorder [11], but concentrate on mobile punctual defects like vacancies, third-component impurities and excess particles in off-stoichiometric binary alloys. These belong to the category commonly named annealed disorder. Despite the theoretical suggestion that such kind of disorder should not modify the asymptotic growth-law [12], experiments [10], and numerical simulation studies [12–15] provide evidences for slow growth, either logarithmic growth laws or algebraic laws with small exponents.

A general feature commonly observed during the early-time evolution in systems with annealed defects is the tendency to concentrate the disorder at the domain walls. Indeed, experiments [10,16] and numerical simulations [8,13–15,12,17] reveal that the vacancies and

the excess particles tend to accumulate at the domain walls. This is accompanied by a depletion in the bulk defect concentration, that renders the excess internal energy unsuitable to measure the total amount of interfaces. Only at late times, as the interfaces disappear and the system approaches equilibrium, the annealed defects may dissolve again into the bulk, provided that they display no cooperative phenomena. Simultaneously an overshooting in the bulk order parameter is observed [12,18]. Very recently it has been suggested [12,19,18] that this is a generic effect in ordering dynamics, coming from a subtle competition between non-equilibrium internal energy and non-equilibrium entropy.

In previous [13,14] studies of the diluted square Ising model with nearest neighbors interactions, it was obtained that the effect of a small concentration of vacancies is dramatic, leading to an extremely slow growth described by a logarithmic growth-law [14] or even to a complete pinning [13]. This difference, obtained on the same model in the limit of low vacancy concentration, comes from special features introduced in the coupled dynamics used; that is, the system evolves according to the non-conserved Glauber dynamics but the vacancy concentration is forced to be constant. We notice that in these studies, the vacancies exhibit a natural tendency to cluster. The results obtained in the present work show that the true asymptotic growth behavior is definitively algebraic with effective exponents smaller than the Allen-Cahn value.

Concerning the present scenario for the effect of excess particles in a non-stoichiometric binary alloys with no vacancies, very recently it has been suggested [8] that the existence of effective interactions between diffusing excess particles and those localized at the APB's is crucial in determining the essential time dependence of the growth-law. They showed that when these specific interactions are not present the main assumptions underlying the Allen-Cahn theory are fulfilled. On the other hand there is experimental evidence that small deviations from the stoichiometric composition may provoke drastic modifications in the growth law. It has been reported that the ordering kinetics in $Cu_{0.79}Au_{0.21}$ [10] shows a crossover from the standard Allen-Cahn growth law, for stoichiometric Cu_3Au [10,20], to a logarithmic growth-law. In reference [8] it was suggested that to account for such

behavior, additional interactions to the ones present in the (nearest neighbors) Ising model are needed. Indeed, the authors showed how this can be accomplished by simply extending the interactions to next nearest neighbors. Our main interest here will be to incorporate the effect of such interactions between annealed impurities in a more general framework.

The three-state Blume-Emery-Griffiths (BEG) model is specially adequate for our purposes [21]. For given values of the model parameters (K and L), the third value of the spin variable may represent either a vacancy or an impurity (in particular an excess particle). In the present work we take the asymmetric term $L = 0$ and restrict to the case of vacancies in a stoichiometric binary alloy, so that the additional coupling coming from the interplay between the diffusive motion of both vacancies and excess particles is not considered here.

The influence of mobile vacancies on the kinetics of ordering arises from the coupling between their diffusive dynamics and the motion of the domain walls (in this case, antiphase-domain boundaries (APB)). This intercoupling depends on the two facts concerning the behavior of the vacancies: their tendency to precipitate into the APBs and their tendency to cluster. Whereas the former is encountered for all values of the model parameters considered here, the interaction among vacancies, and furthermore their tendency to cluster, depends on K . The combination of both effects gives rise to an effective interaction (controlled by K) between bulk diffusing vacancies and those localized at the interface that turns out to be crucial in determining the essential time dependence of the growth-law.

The organization of the paper is the following. We start by defining the model and the region of parameters of interest here (section II). In section III we provide the details of the simulations and describe the algorithms used. In section IV we present the results and discuss them in section V. Finally, in section VI we summarize our main conclusions.

II. THE MODEL AND PARAMETERS

We assume an underlying rigid square lattice with $i = 1, \dots, N = l \times l$ sites that can be occupied either by A -atoms ($S_i = 1$), B atoms ($S_i = -1$) or vacancies ($S_i = 0$). Following

standard procedures, the interactions are taken to be pair-wise and restricted to nearest-neighbors (n.n.) only. The spin-1 BEG hamiltonian is:

$$\mathcal{H} = J \sum_{i,j}^{n.n.} S_i S_j + K \sum_{i,j}^{n.n.} S_i^2 S_j^2 + L \sum_{i,j}^{n.n.} (S_i^2 S_j + S_i S_j^2) \quad (1)$$

where, J stands for the atom-atom ordering interaction, K is a biquadratic coupling parameters accounting for the energy difference between atom-atom pairs and those involving vacancies, and L is an asymmetry term accounting for the energy difference between $A - A$ and $B - B$ pairs. When the parameter K promotes the formation of atom-atom pairs, the vacancies tend to cluster whereas if the vacancy-atom pairs are preferred, cooperative effects for the vacancies are not expected, at least in the limit of low vacancy concentration.

Although the hypothesis of a rigid lattice is crude, since lattice deformations have an strong influence on the dynamics of the atoms around the vacancies, this effect is partially taken into account in the phenomenological character of the constant K . We also expect that the assumption of pair interactions only, disregarding many body effects, only introduces quantitative but not qualitative changes concerning the ordering dynamics.

We have restricted the present study to concentrations so that the system corresponds to a stoichiometric binary alloy with small concentration of vacancies. Since we have taken $J > 0$, the ordered phase will be antiferromagnetic-like, with almost all the bonds of the $A - B$ kind.

As we have mentioned in the introduction our goal here is to study the influence of annealed vacancies on the kinetics of domain growth. This influence originates in the interplay between the two following specific interactions: i) the vacancy-APB interaction (here the APB is thought as a sequence of $A - A$ and $B - B$ bonds) and ii) the vacancy-vacancy interaction. When the the vacancy-APB interaction is attractive, the vacancies tend to concentrate at the APBs and therefore the vacancy-vacancy interaction introduces an effective interaction between bulk vacancies and APBs.

Next step is to calculate these specific interactions for the different values of the model parameters. These, obtained from the bond energies expressed with respect the energy of the

$A - B$ bond, are summarized in Table I. For notation we introduce the following reduced parameters $K^* = K/J$, $L^* = L/J$, with $J > 0$. It follows that $K^* = 1$ separates the tendency for the vacancies to cluster ($K^* < 1$) or not ($K^* > 1$). Moreover, for $|L^*| < 1$ the specific interaction between vacancies and APB's is attractive, favoring the absorption of vacancies at the interfaces. For values of $|L^*| > 1$ the behavior is more complex, in particular, if $K^* < 1$ a competition between K^* and the asymmetric term L^* appears.

The results of the above analysis are illustrated in Fig. 1. We have indicated, in white, the region where the vacancies exhibit tendency to accumulate in the APB's. The line at $K^* = 1$ separates the regions with vacancy attraction and vacancy repulsion. Black circles indicate the points studied in the present work, all sitting along the line $L^* = 0$. The point at $K^* = 0$ and $L^* = 0$ (indicated by an square) has been previously studied in [14] and corresponds to a diluted Ising model. The points with $K^* = 1$ and $L^* = \pm 1$, indicated by diamonds, correspond to a non-stoichiometric binary alloy without vacancies [8].

It is worth mention that the BEG-model, with $K = 0$, $L = 0$ and $J > 0$, has also been used for the study of the ordering dynamics via vacancies with $c_V < 4 \cdot 10^{-4}$. Such a restricted dynamics, only allowing exchanges between atoms and vacancies may strongly modify the dynamics [24]. Such mechanism is not considered in the present study.

III. MONTE CARLO SIMULATIONS

We have performed different Monte Carlo simulations of the model defined in section II with $L^* = 0$, $J > 0$ and K^* inside de range $-0.5 < K^* < 1.4$. First we need to know, in the region of vacancy attraction ($K^* < 1$), the temperature at which the system separates into two phases. This is important in order to characterize the equilibrium state at the point to which quenches have been performed. Next, in order to characterize the time evolution of the ordering process subsequent to the quench, we focus on the study of the structure factor width. It is known that the structure factor provides an overall description of the ordering process. In particular, the study of its time evolution will provide information about the

dynamical scaling properties. These second group of simulations constitute the major part of results presented and, contrarily to the equilibrium simulations, are very time consuming.

A. Equilibrium Simulations: Phase Diagram.

In order to obtain the phase diagram of model (1) in the particular case of $L^* = 0$, we have performed Monte Carlo simulations in the Grand Canonical Ensemble using the Legendre transformation:

$$\mathcal{H}_{GC} = \mathcal{H} - \mu \sum S_i^2 \quad (2)$$

Where μ stands for the chemical potential difference between atoms (either A or B) and vacancies. This is because we restrict to the case of stoichiometric composition ($N_A = N_B$) and the chemical potentials of A and B are then equal. The simulations have been performed on a system of linear size $l = 128$ using the Glauber dynamics implemented into the Metropolis algorithm. The different runs are extended up to 1500 Monte Carlo steps per site (MCs), our unit of time.

Figures 2(a) and (b) show two different sections of the phase diagram. Fig. 2(a) (Temperature *vs.* vacancy concentration) corresponds to a section with fixed $K^* = 0$, and Fig. 2(b) (Temperature *vs.* K^*) to a section with fixed vacancy concentration $c_V = 0.06$. Phase *I* corresponds to an atomic disordered phase with randomly diluted vacancies; phase *II* corresponds to an atomic ordered AB phase with randomly diluted vacancies, which exhibit only short range order; phase *III* corresponds to a phase separation region with coexisting ordered AB domains with low concentration of vacancies and vacancy clusters with a low concentration of disordered atoms. In order to limitate the range of model parameters to be explored in the Monte Carlo simulations we first obtained a qualitative phase diagram using standard Mean-field techniques. For completeness, both results are simultaneously presented in Fig. 2.

B. Non Equilibrium simulations

Although most of the results, presented in the next section, have been obtained following the standard Kawasaki dynamics, alternative optimized algorithms have been used when specially long simulations were needed. This subsection is devoted to the description of the different algorithms used in the study of the time evolution of the process that follows a thermal quench from very high temperature (disordered phase) to $T = 0.1J/k_B$ performed on a stoichiometric binary alloy with a small concentration of vacancies fixed at $c_V = 0.06$ (being $c_A = c_B = 0.47$). The different values of K^* studied correspond to final states into the ordered phases either *II* and *III*.

1. **Standard dynamical simulations.** These are simulations performed using the standard Metropolis algorithm together with the Kawasaki dynamics. The linear system size is $l = 200$ even though some initial studies were performed on systems of $l = 100$. Starting from an initial disordered configuration, the runs have been (typically) extended up to $20000MCs$. Moreover, averages over about 20 independent realizations have been performed. From each simulation we have extracted the time evolution of the structure factor defined as:

$$S(\vec{k}) = \left| \frac{1}{N} \sum_{i=1, N} S_i \exp \left\{ i \frac{2\pi}{a} \vec{k} \vec{r}_i \right\} \right|^2 \quad (3)$$

where \vec{k} are the reciprocal space vectors, a is the lattice parameter and \vec{r}_i is the vector position of site i . We have focused on the profiles along the (10) and (11) directions around the superstructure peak at $\vec{k} = (\frac{1}{2}\frac{1}{2})$. Moreover, they have been averaged over equivalent directions. The size and shape of the ordered domains has been obtained by fitting the averaged profiles to a lorentzian function powered to 3/2 in order to reproduce the Porod's law for the decay of the tail at long q 's [22]:

$$S(q, t) = \left\{ \frac{a(t)}{1 + \left[\frac{q}{\sigma(t)} \right]^2} \right\}^{\frac{3}{2}} \quad (4)$$

where q is the distance to the superstructure peak $q = |\vec{k} - (\frac{1}{2}, \frac{1}{2})|$, $a(t)$ is the height of the peak and $\sigma(t)$ the width. Only data with $S(q, t) > S_0 = 2.5 \cdot 10^{-5}$ has been considered for the fits. S_0 has been obtained from a completely disordered system with the same concentration of particles and vacancies. The quantities $a(t)$ and $\sigma(t)$ provide information about the square order parameter growth and the inverse domains size respectively.

2. **N-fold way algorithm.** For the particular case of $K^* = 0$ and $L^* = 0$ we have used the N-fold way algorithm [23] in order to reach very long times ($10^7 MCs$) in the evolution of a system of linear size $l = 200$. The possible dynamic exchanges have been classified in 11 classes according to their energy change. (A class including the exchanges not affecting the system configuration has also been taken into account, in order to compare with the standard dynamical simulations in which time is spent in such exchanges). The time increment after each exchange has been taken as the expected time that, in a standard Monte Carlo simulation, would pass until a useful proposed exchange be accepted. In this case, structure factor evolution has also been monitored, as explained in the previous case. The averages have been performed over independent runs (~ 30).
3. **Optimized multigrid algorithm.** Given that for the more general case of $K^* \neq 0$, the number of different energy classes is large, the N-fold way algorithm is difficult to construct. In this case, a less optimized algorithm but simpler to implement has been constructed in order to reach very long times. Starting from a standard multigrid algorithm [8,14] we have made, for each sublattice, a list of the exchanges whose probability of being accepted is not negligible. When a given sublattice is chosen, only the exchanges present in the list are attempted. The method turns out to be very efficient when the number of attempted exchanges is low. In particular, for the case $K^* = 0.6$ and $L^* = 0$, we have performed simulations up to $10^7 MCs$ with no major difficulties (the linear system size was $l = 200$ again).

IV. DOMAIN GROWTH RESULTS

The Figure 3 shows snapshots of the microconfigurations as they evolve with time after the quench for three different values of parameter K^* ($=0.6, 1.0$ and 1.4). The linear system size is $l = 200$ and the quench temperature $T = 0.1J/k_B$. In this case we have used the standard dynamical algorithm described before. The vacancies are indicated in black while ordered regions are indicated in white. Due to the tendency exhibited by the vacancies to concentrate at the interfaces the antiphase domain structure shows up naturally. The process of absorption of vacancies at the interfaces starts at very early times and follows on until the whole interface network saturates. This initial regime was studied previously [8] for the case of a non-stoichiometric binary alloy. Simultaneously, it was discussed in a more general context and suggested to be a generic effect in ordering dynamics [12,19,18]. In any case, this is a transient, prior to the long time domain growth regime of interest here. Nevertheless, we remark that this phenomenon of vacancy precipitation at the interfaces results of crucial importance in the subsequent evolution (dictated by interface reduction) specially when the interaction between vacancies is switched on ($K^* \neq 1$). We now come back to Fig. 3. Clear differences can be observed in relation to both the orientation of the the antiphase boundaries and the speed of the evolution towards equilibrium. For $K^* = 0.6$ (vacancy attraction), the domains look square-like with the interfaces preferably directed along the (10) direction. In the case of $K^* = 1.4$ (vacancy repulsion), although the domains are square-shaped as well, the interfaces are directed along the (11) direction. Moreover, in both cases, the interfaces tend to be flat (or almost flat), at least in the regime depicted in Fig. 3. As we shall discuss below, this is a consequence of the vacancy-vacancy interaction which introduces energy barriers for the motion of the vacancies localized at the interfaces favoring, in each case, the different orientation of the APBs. Contrarily, no preferred orientation for the boundaries is observed when $K^* = 1$. Remember that in this case there is no specific interaction between vacancies. Concerning the speed of the different evolutions, the fastest process occurs for $K^* = 1$, whereas for the other two cases it is clearly slower, apparently even more for

$K^* = 1.4$. The introduction of specific interactions between vacancies seems to be behind the slower evolutions, although the underlying physics is different.

Before proceeding further it is interesting to look at the quantitative results obtained from structure factor calculations. In Fig. 4 we show the time evolution peak width $\sigma(t)$ of the structure factor along the two relevant directions (10) (open circles) and (11) (filled circles) for the same three selected values of K^* as in Fig. 3. Dashed lines indicate the regions of algebraic domain growth regime and the numbers on top are the fitted values of the kinetic exponents. We obtain that whereas for $K^* = 1$ and $K^* = 1.4$ both, $\sigma_{(10)}$ and $\sigma_{(11)}$, evolve with the same exponent, for $K^* = 0.6$ the two exponents are clearly different. This is indicative of the existence of anisotropic growth and, as we shall discuss later, it is related to the local accumulation of vacancies at the vertices of the interfaces (see Fig. 3). Moreover, while the values of the exponents for $K^* = 1.4$ and $K^* = 0.6$ are definitively smaller than $1/2$, for $K^* = 1$ it is perfectly consistent with the standard Allen-Cahn value. Notice the large *plateau* obtained in the case $K^* = 1.4$. One needs to perform very large simulations before reaching the algebraic growth regime. In fact, we have also obtained such behavior for some values of $K^* < 1$ inside the region $-0.5 < K^* < 0$. In addition, the extension of the *plateau* depends on K^* suggesting it is related to the existence of activated process with energy barriers depending on K^* . These energies increase (but not symmetrically) as one varies K^* from $K^* = 1$, either to $K^* < 1$ or to $K^* > 1$, and in both cases hinder the motion of the vacancies at the vertices of the interfaces. The expression for the associated energy barriers ($E_b^* = E_b/J$) are: $E_b^* = 1 - K^*$, for $K^* < 1$ and $E_b^* = 3(K^* - 1)$, for $K^* > 1$. In Fig. 5 black dots are the times needed to reach the algebraic regime for the different values of K^* . These have been estimated from the simulations as the ending points of the *plateau*. Simultaneously we have plotted (discontinuous lines) the passing-time, defined as $\tau \sim \exp(E_b^*/k_B T)$. As an example, we show the case of $K^* = 0$ (Fig. 6). The evolution up to $\sim 10^7$ MCs has been obtained by following first the standard dynamical simulations (circles) and next, by using the N-fold way algorithm (squares). The arrow indicates the estimated time for the ending point of the *plateau*.

We have tested the existence of dynamical scaling. Figures 7(a), (b) and (c) show the scaled structure factor profiles. Those along direction (10) have been shifted downwards four decades in order to clarify the picture. Profiles along each direction have been conveniently scaled with the corresponding σ . The overlap of the data is satisfactory except for the tails at large q 's. Nevertheless, to prove the existence of dynamical scaling it is necessary to have not only the collapse of the curves but also one requires that both lengths, $\sigma_{(10)}$ and $\sigma_{(11)}$, evolve with the same power-law. This happens to be the case for $K^* = 1$ and $K^* = 1.4$ whereas for $K^* = 0.6$ both sets of profiles scale independently according to widths evolving with different power-laws.

In the following two figures we present a complete study of both the anisotropic character of the growth and the kinetic growth exponent(s) for a wide range of values of the interaction parameter K^* . Fig. 8 shows the time evolution of the ratio $\eta \equiv \sigma_{(11)}/\sigma_{(10)}$ for different values of K^* . For $K^* < 0.8$, η definitively increases with time, showing that the shape of the ordered domains becomes more and more spike-like. For $0.8 < K^* < 1.0$ the ratio η remains constant indicating that the domains are circular during all the evolution. For $K^* > 1$ after an initial decrease, η reaches the value $1/\sqrt{2}$ indicating that, at large times, the domains are square-like and grow isotropically.

Figure 9 shows the growth exponents obtained by fitting an algebraic growth law to the evolution of both $\sigma_{(10)}$ (open circles) and $\sigma_{(11)}$ (filled circles). Note that Allen-Cahn values ($n \simeq 0.5$) are only reached for values of $K^* \sim 1$.

We have also studied the behavior of the structure factor at large q 's. They are affected by two different phenomena. (i) Along the direction (1, 1) for $q > 0.5$ the structure factor is distorted due to the existence of the non-scaling fundamental peak at $\vec{k} = (00)$. (Strictly speaking the value of the structure factor at $\vec{k} = (00)$ is always zero, but the peak exhibits some finite width due to the existence of disorder in the system) (ii) For the cases in which the vacancies dissolve into the bulk, there is an homogeneous non-scaling background which, in turn, may evolve in time.

V. DISCUSSION

The differences in the values obtained for the kinetic exponent of the growth law lie on the different characteristics of the intercoupling between bulk diffusing vacancies and the interface motion. For $K^* \neq 1$ this intercoupling proceeds via an effective interaction originated from the vacancy-vacancy specific interaction. Moreover, this introduces differences in the internal structure of the interface. In the particular case of $K^* = 1$, this intercoupling reduces to a simple encounter between curvature-driven interfaces and mobile vacancies which mutually cross their respective trajectories. This does not make the curvature ineffective but may slow down the domain growth. It has been shown that [8] the effect of this simple intercoupling does not modify the essential time dependence of the growth law but modifies the growth rate (prefactor) which decreases as the mobile impurity concentration increases.

We next discuss separately the other two cases. We start with the case of vacancy attraction ($K^* = 0.6$) and point out some other relevant features present in Fig. 3. Notice the increasing concentration of vacancies at the interfaces as they evolve with time. This is premonitory of the phase separation process, eventually reachable at longer times. During the regime showed in Fig. 3 one is mainly concerned with a non homogeneous distribution of vacancies along the interfaces. Special mention deserves the local accumulation at the vertices. This is the signature of a previous fast process of interface reduction (due to the high-curvature of the vertices). The further evolution is hindered until the vacancies diffuse along the interfaces. This involves activated processes. Indeed, in our simulations we have observed how the temporal pinning of the high-curvature portion of the interfaces provokes that the further evolution of the interconnecting interfaces (with lower curvature) does not fulfill the main assumptions underlying the Allen-Cahn theory. The importance of this temporal pinning depends on K^* , since the energy barriers ($E_b^* = 1 - K^*$) for a vacancy at the corner of the interface to move increases as K^* decreases from $K^* = 1$. In Fig. 10 we show this effect for the case $K^* = 0$. In particular, one observes how the single (rectangular) domains evolve so that they become more and more plate-like. This is because

the longer interfaces (with a lower concentration of vacancies) are the only able to evolve. Moreover, they remain (almost) flat and parallel to the (10) direction. This feature is not observed in previous studies on the diluted antiferromagnetic Ising model [14] (notice that it corresponds to the BEG with $K^* = 0$) so that it cannot be attributed exclusively to the interaction (which favors the vacancies to be nearest neighbors at the interface). In Fig. 11 we schematically illustrate this mechanism of evolution. It represents a typical domain in the regime under discussion here; that is, the regime characterized because the width of the interface is small and the only relevant length is the size of the AB ordered domains. Two facts have to be taken into account: the attractive vacancy-vacancy interaction defined by the hamiltonian and the conserved character of the implemented dynamics (Kawasaki). The combination of both introduce energy barriers for the motion of the vacancies (circles) at the interfaces which hinder the shrinkage of the domain. We have indicated in black (white) the vacancies with associated energy barriers so that they are induced to go outwards (inwards). The vacancies in grey do not have any preference. The crucial point is that the motion inwards of the vacancies at the corner are strongly hindered whereas for its neighbors, it is favored. This provokes that the shrinkage of the domains proceeds by displacing the flat interfaces and accumulating the excess vacancies at the vertices [25]. The domains become then spike-like along the (11) direction breaking down the single-length dynamical scaling and so the growth is anisotropic. In reference [14], the authors coupled the Glauber dynamics for the spins to the conserved dynamics for the number of vacancies in such a way that the vacancy at the corner is not pinned. Nevertheless they found that the dynamical evolution of the ordering process is effectively described by a logarithmic growth-law (in the limit of low vacancy concentration). Other studies [13] on the diluted ferromagnetic Ising model, encountered that, by coupling both dynamics differently (the simultaneous vacancy-spin exchange and spin flip is not allowed) so that the vacancy at the corner is effectively pinned, the growth stops. In the case of the alloy, the dynamics implemented follows directly from the requirement of the conservation law for the number of particles and we found that the ordering process is definitively described by a growth-law that although being slower than

the Allen-Cahn law it is definitively algebraic. For some values of K^* this algebraic regime is preceded by a *plateau* with extension depending on K^* . More precisely, it is larger as bigger the energy barriers are. In particular, we found that for $K^* = 0$ this algebraic regime is visible only after $\sim 10^5$ MCs (see Fig. 6). We notice that the BEG model, in the particular case of $K = L = 0$, corresponds to a diluted Ising model. In view of this, we believe that the growth-law for the diluted antiferromagnet is algebraic. In fact, the authors in [14] did not excluded this possibility in their discussion. Concerning, the complete pinning of the process reported by [13], it is certainly due to the extremely low temperature.

Later on, as the width of the interface increases, this pinning effect, localized at the corner, becomes less important and one expects the system crosses over to a complete different regime. In this asymptotic regime, not reached in our simulations, to talk about the interface, as formed by the increasing accumulation of vacancies, is meaningless. Rather, one would deal with a phase-separation process which is not studied in the present work.

We now focus on the discussion for $K^* = 1.4$. In this case, the repulsive interaction between vacancies favors them to be next nearest neighbors at the interfaces. As previously, the driving force is contained in the corner but its motion is hindered by a barrier of energy $2(K^* - 1)$. The interface connecting two vertices is directed along the (11) direction and evolves so that it displaces parallelly. The energy barrier associated to this mechanism is $E_b^* = 3(K^* - 1)$. The vacancies, in excess as a consequence of the interface reduction, are in this case (vacancy repulsion) expelled to the bulk. Moreover, the migrating interface has to cope with the effective repulsive interaction with the bulk vacancies, which concentration increases as the system evolves. Indeed, one expects this should interfere the dynamics. At this point, it is interesting to discriminate whether or not this interference makes the curvature-driven mechanism to become ineffective. In this sense, we have verified that the interface evolves covering a domain area constant in time. This is shown in Fig. 12 for single domains directly extracted from our simulations. These calculations have been performed using the optimized multogrid algorithm discussed previously. A linear time dependence for the domain area evolution is obtained. This is commonly accepted to be indicative that

the motion of the interface is curvature-driven [26]. It then follows that the effect of the intercoupling between mobile bulk vacancies and the evolving interfaces is, in this case, to slow down the global process as it is revealed by a decreasing in the effective growth exponent but it does not make ineffective the curvature driven mechanism which remains as the underlying mechanism for the motion of the interfaces. Moreover the effective exponent tends to the ideal $1/2$ -Allen-Cahn value as $K^* \rightarrow 1$.

VI. SUMMARY

We use a Blume-Emery-Griffiths model (with $L = 0$) to study the influence of mobile vacancies in the kinetics of domain growth in a stoichiometric binary alloy after quenches to very a low temperature ($T = 0.1J/k_B$) through an order-disorder transition. The study is performed by Monte Carlo simulations in the limit of low vacancy concentration for a wide range of values of the biquadratic coupling parameter K^* which controls the specific vacancy-vacancy interaction. For all values of K^* inside the range $-0.5 < K^* < 1.4$ we found that the vacancies tend to concentrate at the interfaces. This feature introduces, via the parameter K^* , an intercoupling between diffusing bulk vacancies and moving interfaces. In the particular case of $K^* = 1$ this intercoupling does not take place via any specific interaction and the ordering process is consistent with the Allen-Cahn law. In fact we find that $n \sim 1/2$ for $K^* \sim 1$ whereas the exponent is clearly smaller when such interaction is present, no matter if it is attractive ($K^* < 1$) or repulsive ($K^* > 1$). Nevertheless, our results clearly show that the growth is definitively algebraic. When $K^* < 1$ the attractive vacancy interaction favours the increasing accumulation of vacancies at the interfaces as the system evolves. The regime of interest here corresponds to the very initial stages of a phase separation process when the width of the interfaces is small and the only relevant length is the size of the AB ordered domains. Our main finding is that for quenches inside the coexistence region the growth for the binary alloy is, in this regime, anisotropic. This is related to the existence of energy barriers (depending on K^*) which hinder the motion of the

vacancies at the vertices of the (10) square-like domains and simultaneously provoke local accumulations of vacancies along the (11) directions. Furthermore, these barriers may delay the apparition of the algebraic regime of the growth process to very late times. Concerning the underlying mechanism for the motion of the interfaces, it is not purely curvature driven and the two effective exponents needed to describe the process are lower than the Allen-Cahn value. Nevertheless, both tend to $n = 1/2$ as $K^* \rightarrow 1$. For $K^* > 1$ the specific vacancy-vacancy interaction is repulsive and the interfaces of the square-like domains are in this case directed along the (11) directions. As in the previous case, the motion of the vacancies at the vertices is an activated process. The associated energy barriers depend on K^* and the algebaric growth regime shows up only after the time needed for overpassing the barrier. Since the interface motion has to cope with the repulsive diffusive vacancy interaction, we found that the ordering process clearly slows down. Nevertheless, this repulsion does not make the curvature ineffective. The effective exponent is lower than the Allen-Cahn value but approaches to $n = 1/2$ as $K^* \rightarrow 1$, as it is expected.

ACKNOWLEDGMENTS

We acknowledge financial support from the Comisión Interministerial de Ciencia y Tecnología (CICyT, project number MAT95-504) and supercomputing support from Fundació Catalana per a la Recerca (F.C.R.) and Centre de Supercomputació de Catalunya (CESCA). M.P. and C.F. also acknowledge financial support from the Comissionat per a Universitats i Recerca (Generalitat de Catalunya).

REFERENCES

- [1] *Dynamics of ordering processes in Condensed Matter*, edited by S. Komura and H. Furukawa (Plenum, New York 1988).
- [2] J.D. Gunton, M. San Miguel, and P.S. Sahni, in *Phase Transitions and Critical Phenomena*, edited by C. Domb and J.L. Lebowitz (Academic, New York, 1983), Vol. 8.
- [3] S.M. Allen and J.W. Cahn, *Acta Metall.* **27**, 1085 (1979).
- [4] I.M. Lifshitz and V.V. Slyozov, *J. Phys. Chem. Solids* **19**, 35 (1961).
- [5] M.K. Phani, J.L. Lebowitz, M.H. Kalos and O. Penrose, *Phys. Rev. Lett.* **45**, 366 (1980).
- [6] P.S. Sahni, G. Dee, J.D. Gunton, M. Phani, J.L. Lebowitz and M. Kalos, *Phys. Rev. B* **24**, 410 (1981).
- [7] H.C. Fogedby and O.G. Mouritsen, *Phys. Rev. B* **37**, 5962 (1988), and references therein.
- [8] M. Porta and T. Castán, *Phys. Rev. B* **54**, 166 (1996).
- [9] F. Bley and M. Fayard, *Acta Metall.* **24**, 575 (1976).
- [10] R.F. Shannon, C.R. Harkless and S.E. Nagler, *Phys. Rev. B* **38**, 9327 (1988).
- [11] D.A. Huse and C.L. Henley, *Phys. Rev. Lett.* **54**, 2708 (1985).
- [12] H. Gilhøj, C. Jeppesen and O. G. Mouritsen, *Phys. Rev. E* **52**, 1465 (1995).
- [13] D.J. Srolovitz and G.N. Hassold, *Phys. Rev. B* **35**, 6902 (1987).
- [14] O.G. Mouritsen and P.J. Shah, *Phys. Rev. B* **40**, 11445 (1989); P.J. Shah and O.G. Mouritsen, *Phys. Rev. B* **41**, 7003 (1990).
- [15] O.G. Mouritsen, P.J. Shah and J.V. Andersen, *Phys. Rev. B* **42**, 4506 (1990).
- [16] K. Oki, H. Sagane, and T. Eguchi, *J. Phys. (Paris) Colloq.* **38**, C7-414 (1977).
- [17] T. Ohta, K. Kawasaki, and A. Sato, *Phys. Lett. A* **126**, 93 (1987).

- [18] H. Gilhøj, C. Jeppesen and O. G. Mouritsen, Phys. Rev. E **53**, 5491 (1996).
- [19] H. Gilhøj, C. Jeppesen and O. G. Mouritsen, Phys. Rev. Lett. **75**, 3305 (1995).
- [20] S.E. Nagler, R.F. Shannon, C.R. Harkless, M.A. Singh and R.M. Nicklow, Phys. Rev. Lett. **61**, 718 (1988).
- [21] M. Blume, V. J. Emery, and R. B. Griffiths, Phys. Rev. A **4**, 1071 (1971).
- [22] G. Porod, in *Small Angle X-Ray Scattering*, edited by O. Glatter and L. Kratky (Academic, New York, 1982).
- [23] A.B. Bortz, M.H. Kalos, and J.L. Lebowitz, J. Comp. Phys. **17**, 10 (1975).
- [24] E.Vives and A.Planes, Phys. Rev. Lett. **68**, 812 (1992); Phys. Rev B **47**, 2557 (1993); C.Frontera, E.Vives, and A.Planes, Phys. Rev. B **48**, 9321 (1993).
- [25] If this analysis is done in a circular domain, it can be seen that it first evolves to a square domain and then proceeds as discussed.
- [26] E. Domany and D. Kandel, in *Cellular Automata and Modeling of Complex Physical Systems*, edited by P. Manneville, N. Boccara, G.Y. Vichniac, and R. Bidaux (Springer-Verlag, Berlin, 1990), p.98.

TABLES

TABLE I. Bond energies and the same measured with respect to the $A - B$ bond for the BEG model as a function of the parameters J , K , and L .

Bond	Energy	Excess energy
$A - B$	$-J + K$	0
$A - A$	$J + K + 2L$	$2J + 2L$
$B - B$	$J + K - 2L$	$2J - 2L$
$A - V$	0	$J - K$
$B - V$	0	$J - K$
$V - V$	0	$J - K$

FIGURES

FIG. 1. Regions in the space of the parameters K^* and L^* where different dynamics are expected. The solid line $K^* = 1$ separates the region of vacancy attraction ($K^* < 1$) from the region of vacancy repulsion ($K^* > 1$). The solid lines $L^* = \pm 1$ separates the region where the vacancies tend to precipitate at the antiphase boundaries ($|L^*| < 1$) from the region of vacancy-antiphase boundary repulsion ($|L^*| > 1$). Solid circles indicate the points studied in the present work. The square corresponds to the case $K^* = L^* = 0$ and the diamonds are the points where the model is formally equivalent to a non-stoichiometric binary alloy.

FIG. 2. (a) T vs. c_V phase diagram of the BEG model for $K^* = L^* = 0$. (b) T vs. K^* phase diagram of the BEG model for $L^* = 0$ and $c_V = 0.06$. The points correspond to the Monte Carlo results whereas the solid lines are obtained from mean-field calculations. Dashed lines are just guides to the eyes. In the insert, we show the region of interest. The arrows indicate the working temperature and vacancy concentration

FIG. 3. Snapshots of the evolving domain structure for $K^* = 0.6$, $K^* = 1.0$ and $K^* = 1.4$. Vacancies (A and B particles) are painted in black (white). The simulations are performed in a 200×200 square lattice with $c_V = 0.06$ at $T = 0.1J/k_B$.

FIG. 4. Width of the structure factor, σ , vs. time for $K^* = 0.6$, $K^* = 1.0$ and $K^* = 1.4$. Open circles correspond to the (10) direction and filled circles to the (11) direction. Dashed lines indicate the regions where the growth exponents, written on top, are fitted.

FIG. 5. Time needed to reach the algebraic regime vs. K^* (black circles). Dashed lines are the predicted slopes of these curves from the energy barriers present in the model.

FIG. 6. Structure factor width, σ , *vs.* time for $K^* = 0$. Open/filled symbols correspond to the (10)/(11) direction. The end of the *plateau* is taken to be at the inflection point, as indicated by the arrow. The results shown by circles have been obtained following standard simulations whereas the long time results, indicated by squares, have been obtained by using the N-fold way algorithm. The system size is 200×200 , $c_V = 0.06$ and $T = 0.1J/k_B$.

FIG. 7. log-log plot of the scaled structure factor profiles in the (10) and (11) directions for $K^* = 0.6$, $K^* = 1.0$ and $K^* = 1.4$. The profiles in the (10) direction have been shifted four decades below in order to clarify the picture.

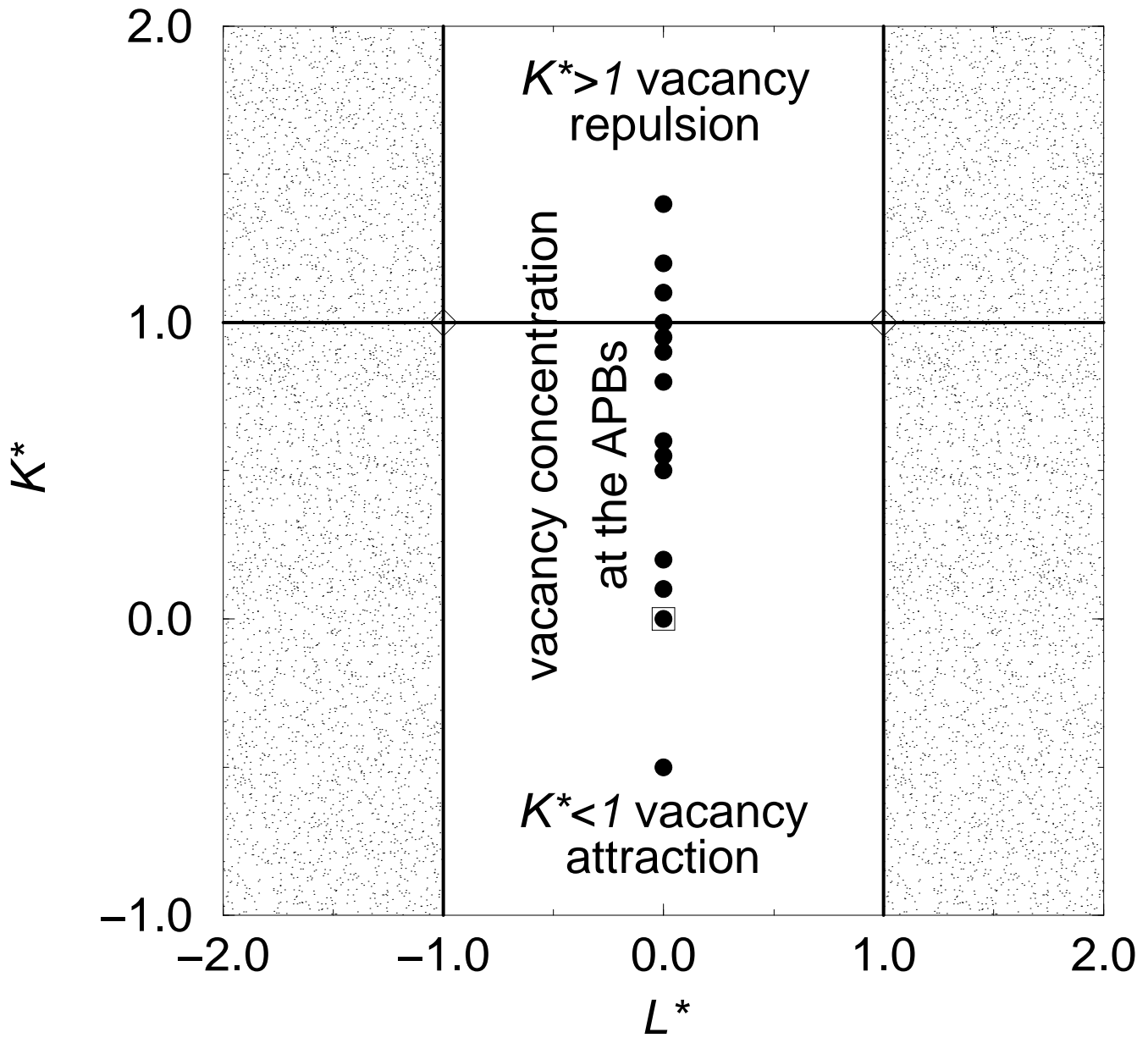
FIG. 8. Ratio $\eta \equiv \sigma_{(10)}/\sigma_{(11)}$ *vs.* time for different values of the parameter K^* . All these simulations are performed in a 200×200 square lattice with $c_V = 0.06$ at $T = 0.1J/k_B$.

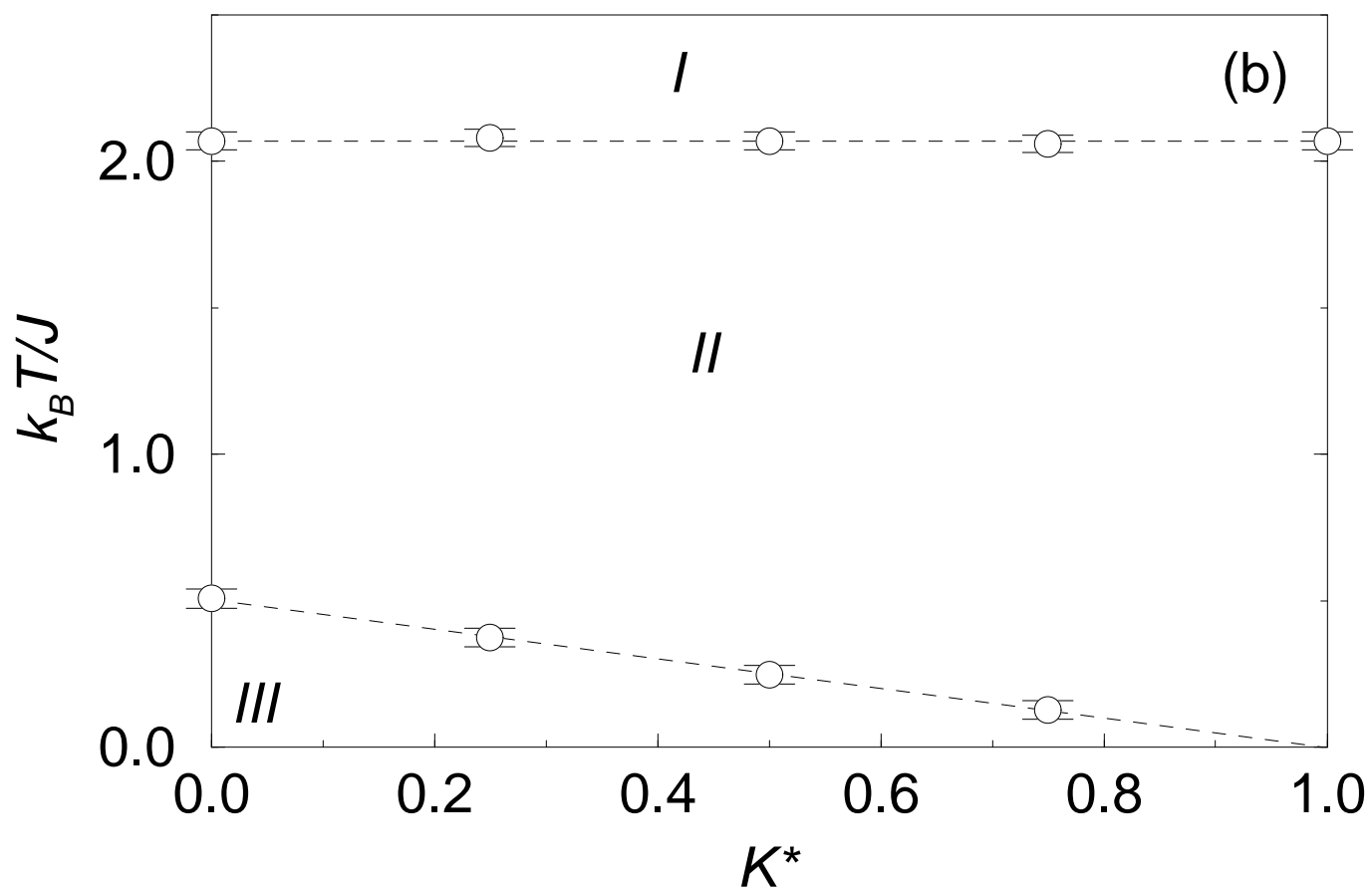
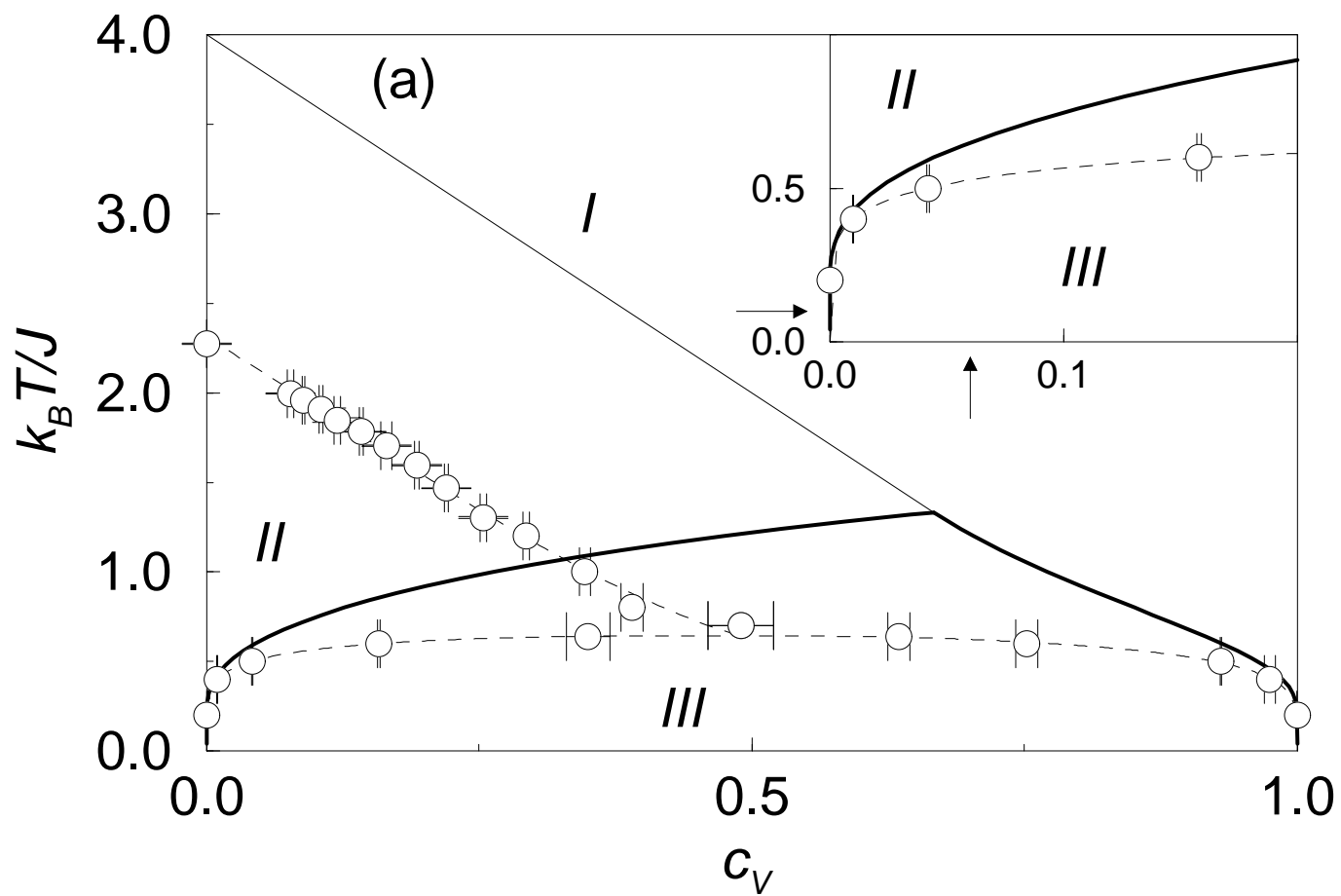
FIG. 9. Growth exponent, *vs.* K^* obtained from the structure factor width, σ . Open (filled) circles correspond to the evolution of $\sigma_{(10)}$ ($\sigma_{(11)}$). All the simulations are performed in a 200×200 square lattice with $c_V = 0.06$ at $T = 0.1J/k_B$.

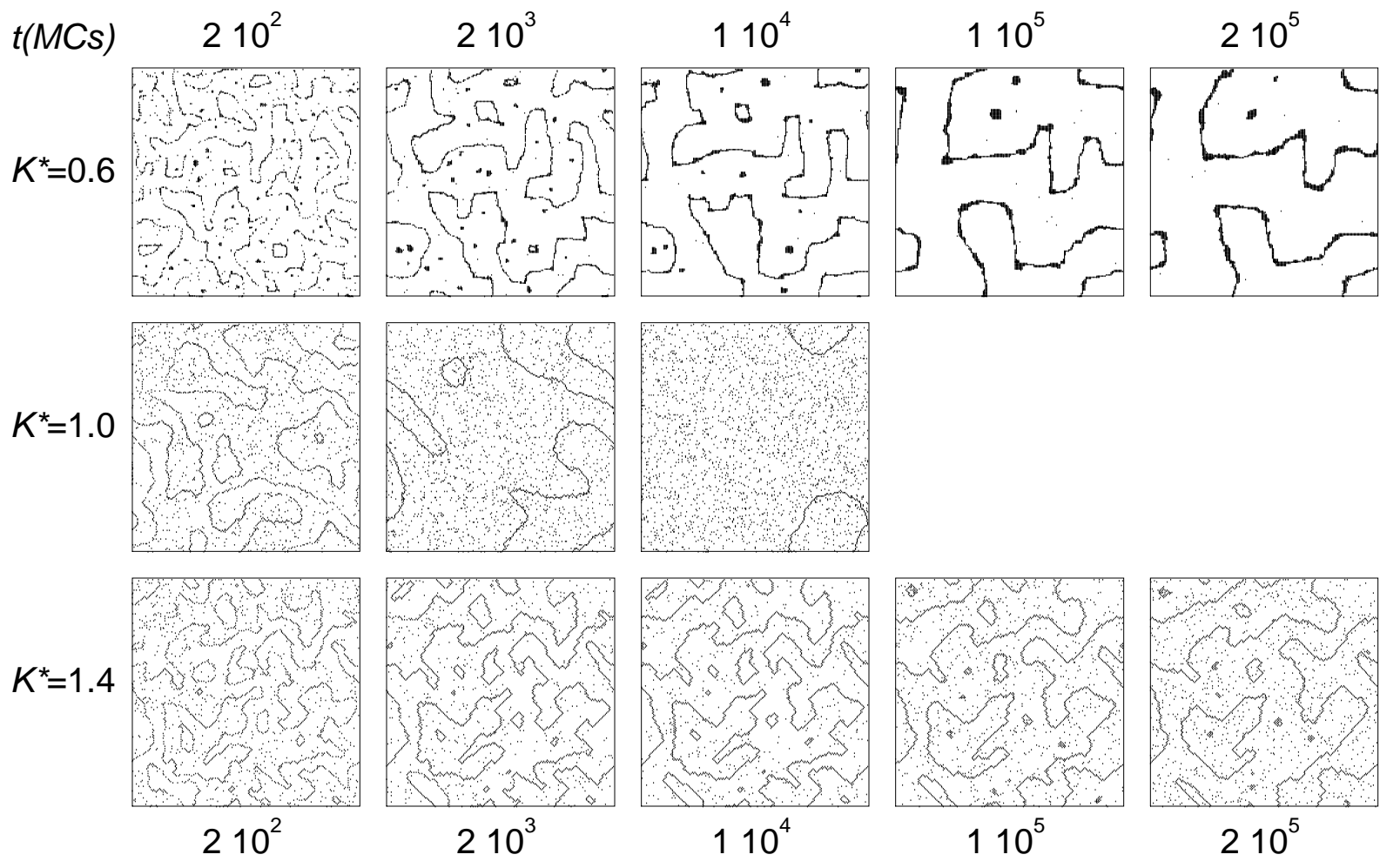
FIG. 10. Snapshots of some evolving domains directly extracted from our simulations for $K^* = 0$. Vacancies (*A* and *B* particles) are painted in black (white). The simulations are performed in a 200×200 square lattice with $c_V = 0.06$ at $T = 0.1J/k_B$.

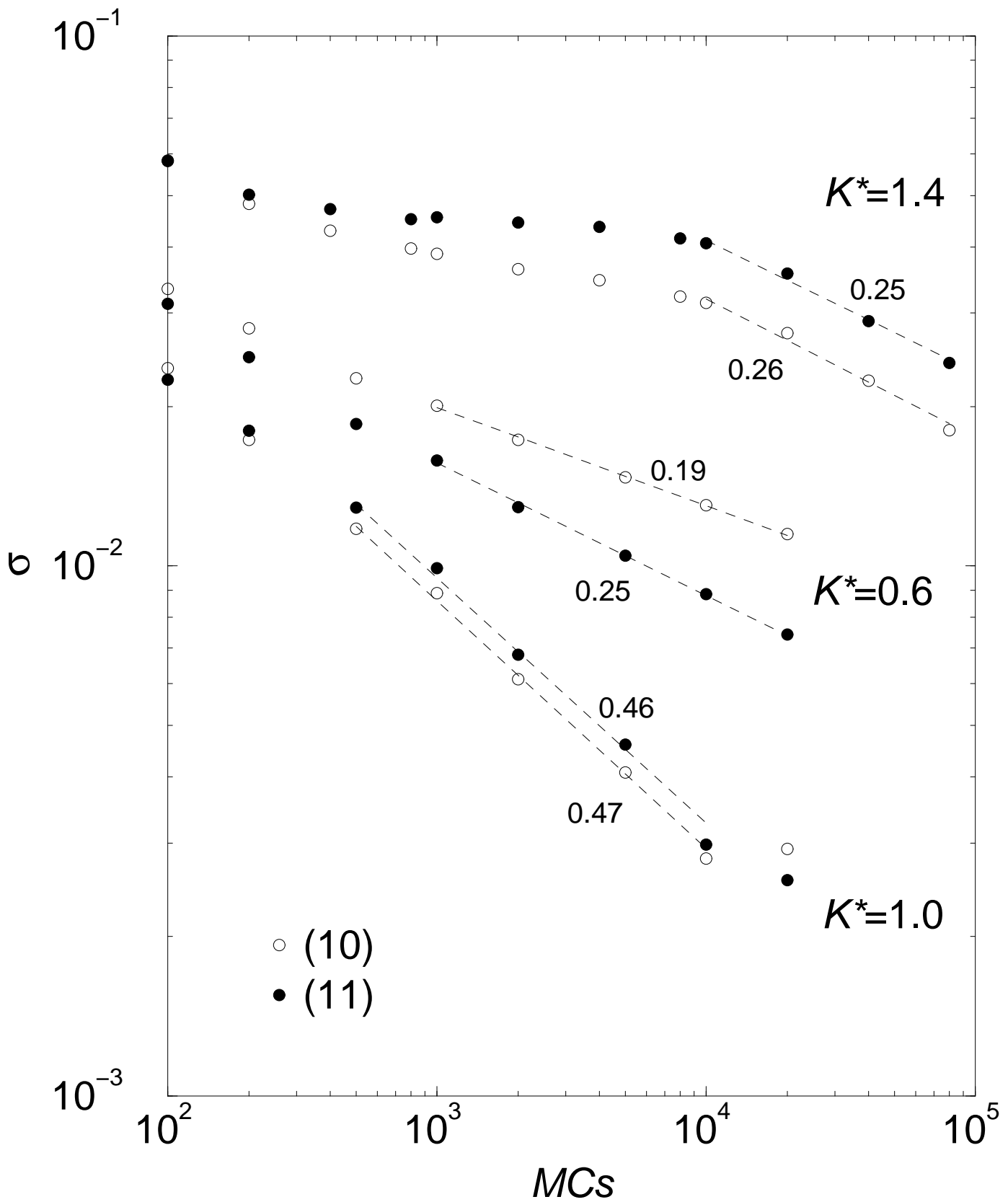
FIG. 11. Schematic representation of the evolution of a square domain typically observed in the $K^* < 1$ simulations. The circles represent vacancies whereas the white (black) squares represent *A* (*B*) particles. The mechanism of evolution is emphasized by painting in black (white) those vacancies which have the tendency to move outwards (inwards). The vacancies painted in grey are the ones which are, in this sense, indifferent.

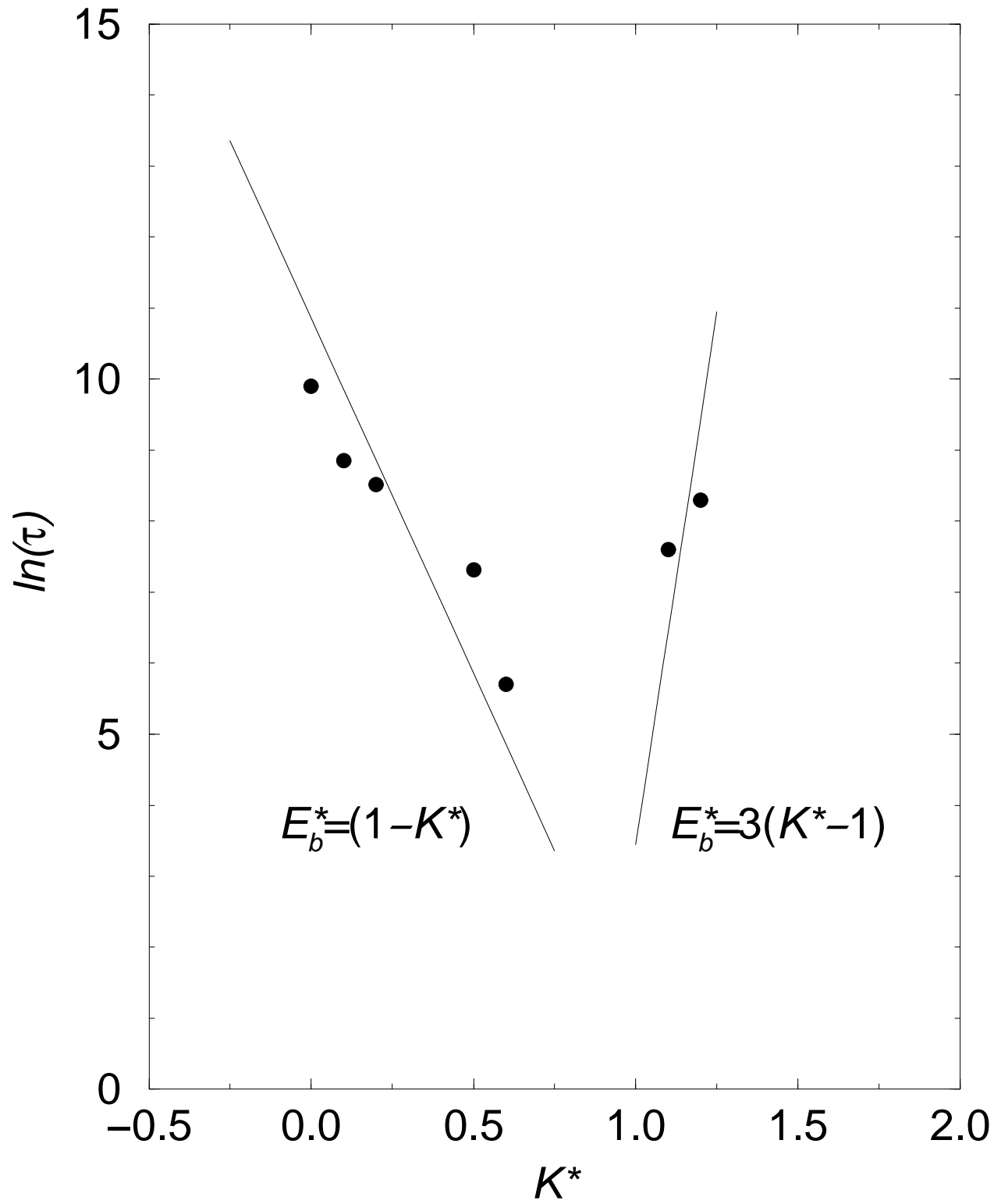
FIG. 12. Domain area *vs.* time of a single domain for $K^*=1.2$ (solid and dotted lines) and $K^* = 1.4$ (dashed line). The solid (dotted) line corresponds to $c_V=0.06$ ($c_V=0.04$). We simultaneously show, in the inset, the time evolution of the total amount of bulk vacancies in the system. The simulations are performed in a 200×200 square lattice at $T = 0.1J/k_B$.

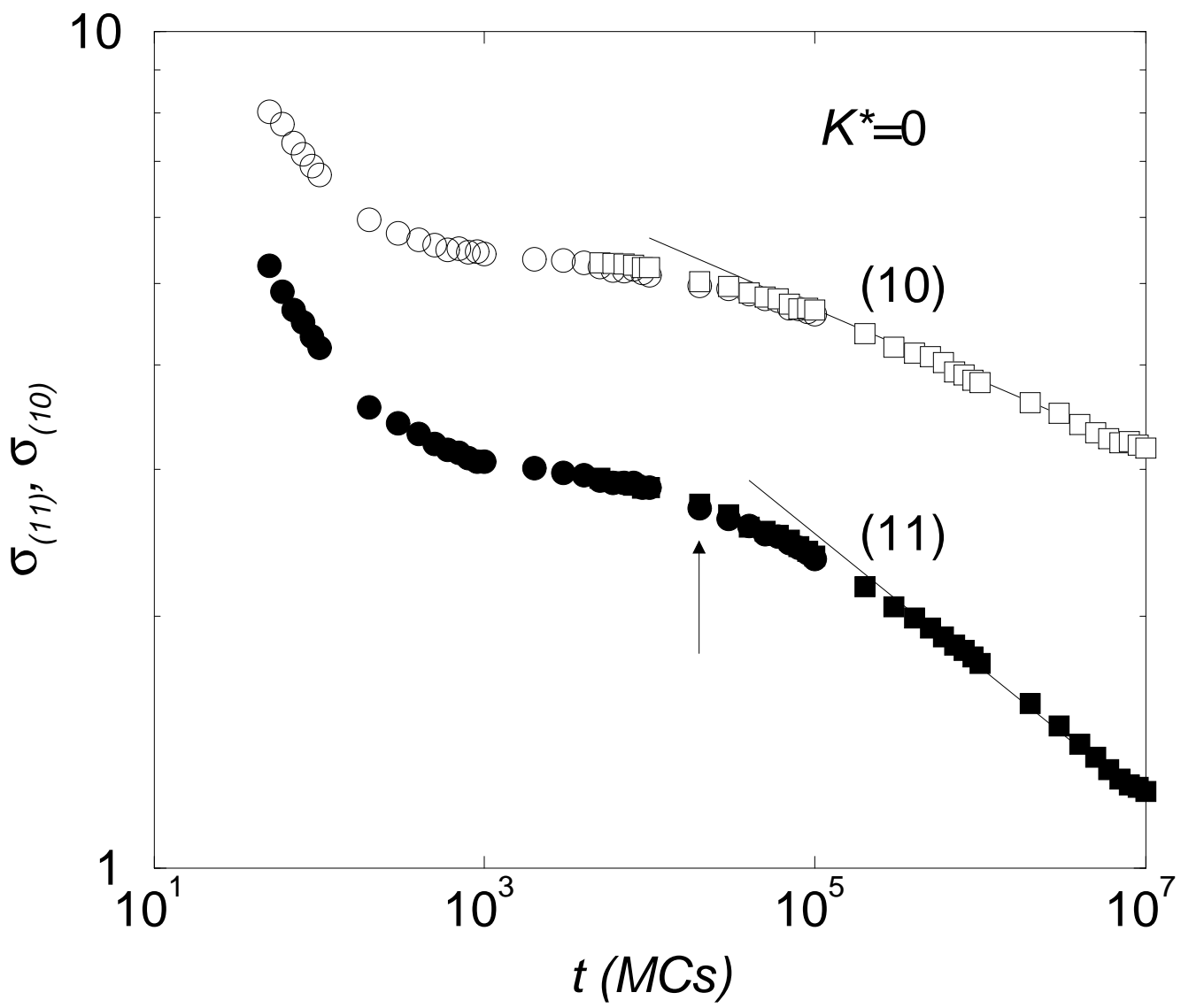


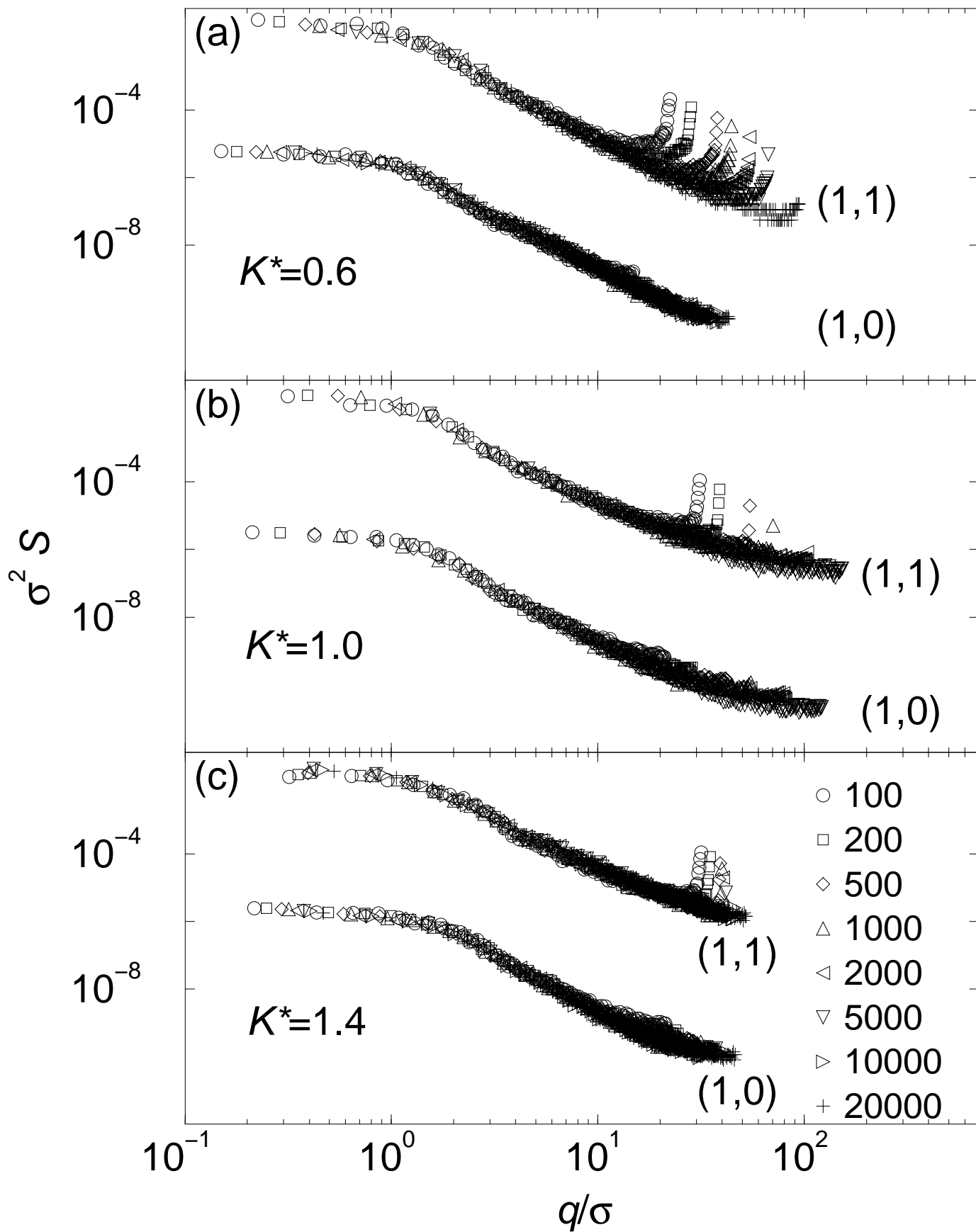


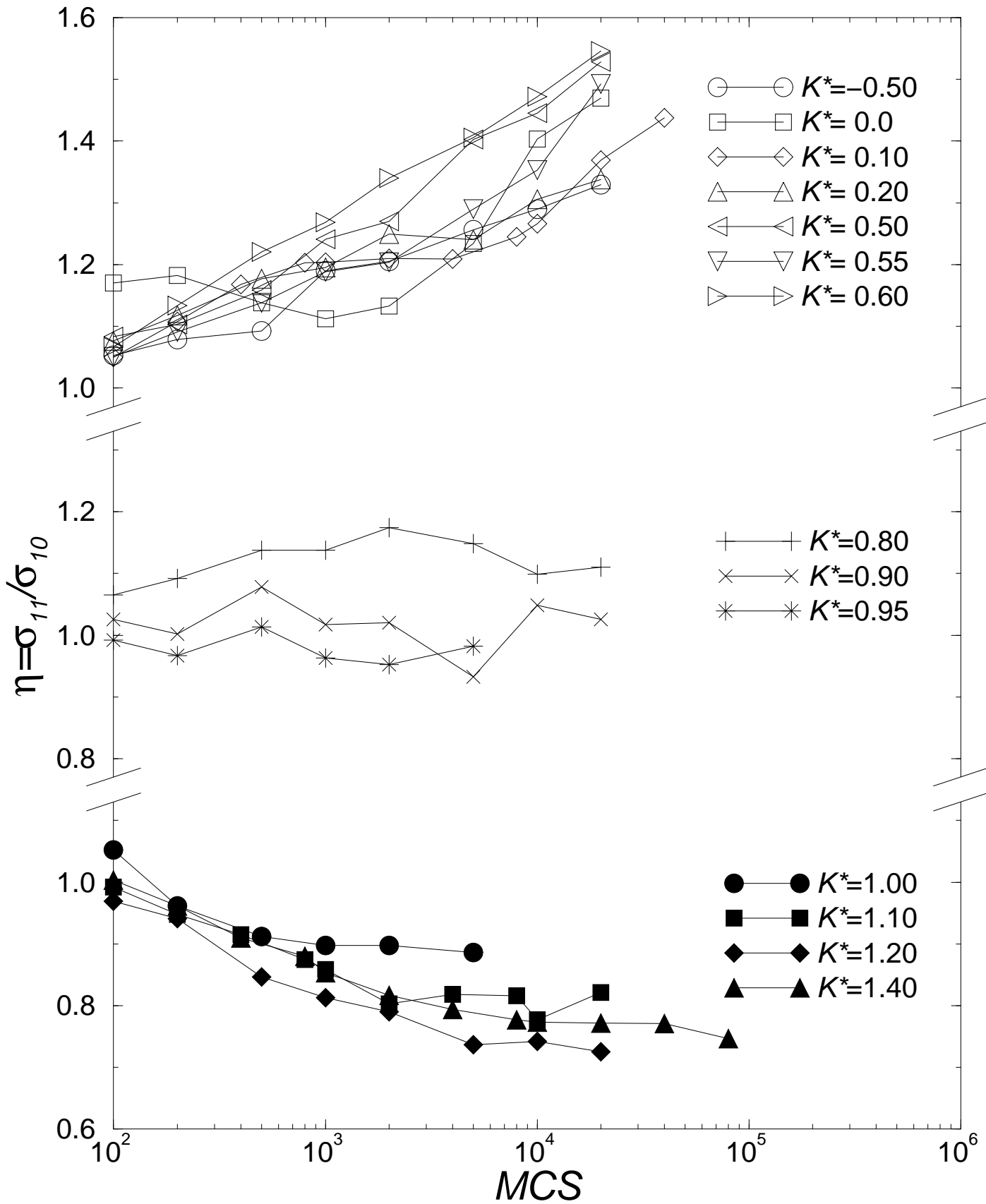


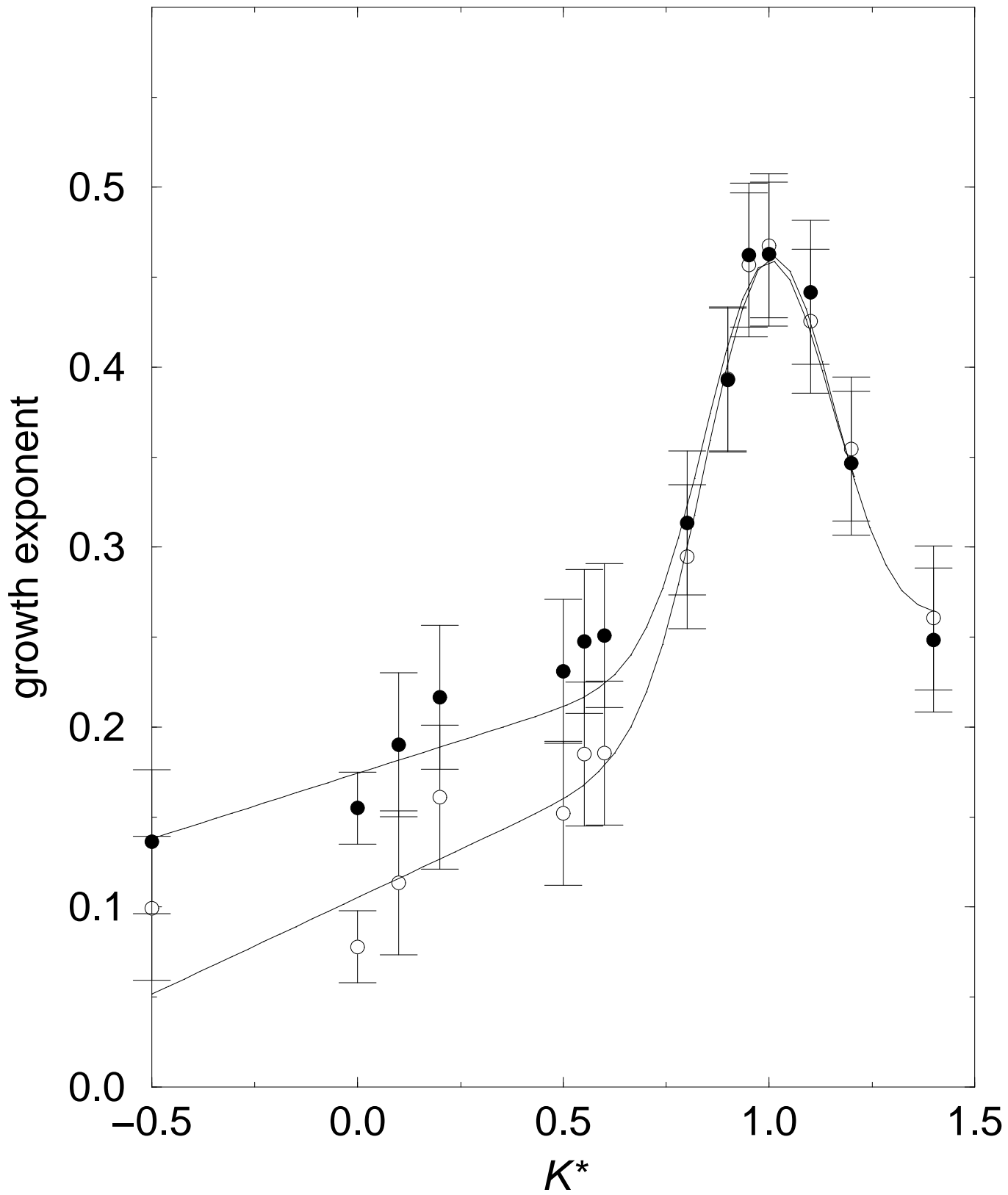












$t(\text{MCs})$

10^6

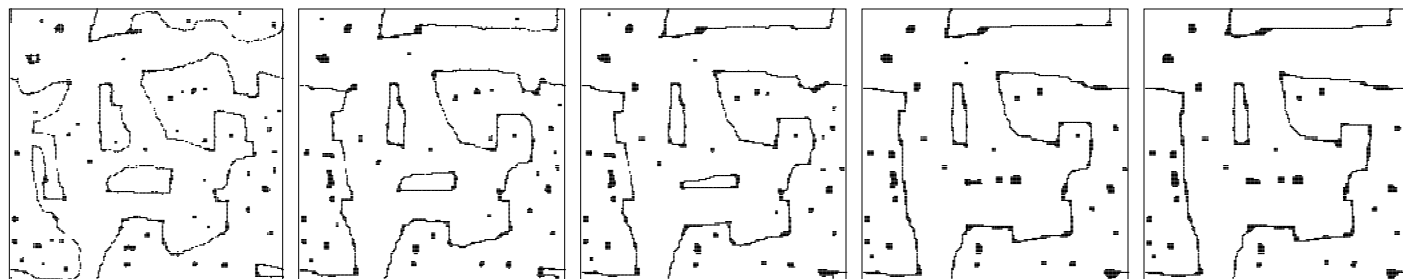
$5 \cdot 10^6$

10^7

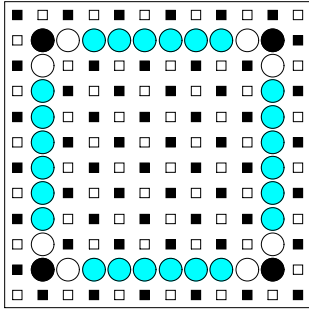
$5 \cdot 10^7$

10^8

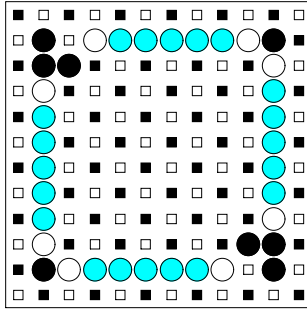
$K^*=0$



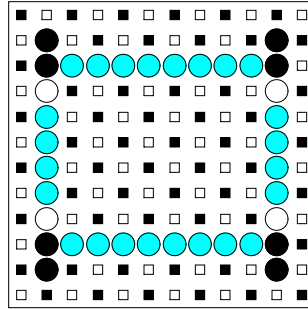
(a)



(b)



(c)



(d)

